Atmos. Chem. Phys., 16, 9533–9548, 2016
www.atmos-chem-phys.net/16/9533/2016/
doi:10.5194/acp-16-9533-2016

Atmospheric Chemistry and Physics Open Access EGU

Co-benefits of global and regional greenhouse gas mitigation for US air quality in 2050

Yuqiang Zhang[1], Jared H. Bowden[1], Zachariah Adelman[1,2], Vaishali Naik[3], Larry W. Horowitz[4], Steven J. Smith[5], and J. Jason West[1]

[1]Environmental Sciences and Engineering Department, University of North Carolina at Chapel Hill, Chapel Hill, NC 27599, USA
[2]Institute for the Environment, University of North Carolina at Chapel Hill, Chapel Hill, NC 27599, USA
[3]UCAR/NOAA Geophysical Fluid Dynamics Laboratory, Princeton, NJ 08540, USA
[4]NOAA Geophysical Fluid Dynamics Laboratory, Princeton, NJ 08540, USA
[5]Joint Global Change Research Institute, Pacific Northwest National Laboratory, College Park, MD 20740, USA

Correspondence to: J. Jason West (jjwest@email.unc.edu)

Received: 27 December 2015 – Published in Atmos. Chem. Phys. Discuss.: 21 January 2016
Revised: 13 June 2016 – Accepted: 2 July 2016 – Published: 1 August 2016

Abstract. Policies to mitigate greenhouse gas (GHG) emissions will not only slow climate change but can also have ancillary benefits of improved air quality. Here we examine the co-benefits of both global and regional GHG mitigation for US air quality in 2050 at fine resolution, using dynamical downscaling methods, building on a previous global co-benefits study (West et al., 2013). The co-benefits for US air quality are quantified via two mechanisms: through reductions in co-emitted air pollutants from the same sources and by slowing climate change and its influence on air quality, following West et al. (2013). Additionally, we separate the total co-benefits into contributions from domestic GHG mitigation vs. mitigation in foreign countries. We use the Weather Research and Forecasting (WRF) model to dynamically downscale future global climate to the regional scale and the Sparse Matrix Operator Kernel Emissions (SMOKE) program to directly process global anthropogenic emissions to the regional domain, and we provide dynamical boundary conditions from global simulations to the regional Community Multi-scale Air Quality (CMAQ) model. The total co-benefits of global GHG mitigation from the RCP4.5 scenario compared with its reference are estimated to be higher in the eastern US (ranging from 0.6 to 1.0 $\mu g\,m^{-3}$) than the west (0–0.4 $\mu g\,m^{-3}$) for fine particulate matter ($PM_{2.5}$), with an average of 0.47 $\mu g\,m^{-3}$ over the US; for O_3, the total co-benefits are more uniform at 2–5 ppb, with a US average of 3.55 ppb. Comparing the two mechanisms of co-benefits, we find that reductions in co-emitted air pollutants have a much greater influence on both $PM_{2.5}$ (96 % of the total co-benefits) and O_3 (89 % of the total) than the second co-benefits mechanism via slowing climate change, consistent with West et al. (2013). GHG mitigation from foreign countries contributes more to the US O_3 reduction (76 % of the total) than that from domestic GHG mitigation only (24 %), highlighting the importance of global methane reductions and the intercontinental transport of air pollutants. For $PM_{2.5}$, the benefits of domestic GHG control are greater (74 % of total). Since foreign contributions to co-benefits can be substantial, with foreign O_3 benefits much larger than those from domestic reductions, previous studies that focus on local or regional co-benefits may greatly underestimate the total co-benefits of global GHG reductions. We conclude that the US can gain significantly greater domestic air quality co-benefits by engaging with other nations to control GHGs.

1 Introduction

Climate change and air quality are interrelated problems. First, climate change can affect the formation, destruction and transport of major air pollutants, through changes in the meteorological variables of temperature, precipitation, air stagnation events, etc. (Weaver et al., 2009; Jacob and Winner, 2009; Fiore et al., 2012, 2015). It can also affect natural

emissions (biogenic gases and particles, dust, fire and lighting) that influence air quality. Second, air pollutants such as particulate matter (PM) and ozone (O_3) can change the climate by altering the solar and terrestrial radiation balance through direct and indirect effects (Myhre et al., 2013). Third, the sources of emissions of greenhouse gases (GHGs) and air pollutants are usually shared, particularly through the combustion of fossil fuels, so actions to control one can also influence emissions of the other. Policies to control GHG emissions will therefore not only slow climate change in the future but will also provide co-benefits of improvements to air quality and consequently to human health (Bell et al., 2008; Nemet et al., 2010).

Recent studies that model future air quality have focused on the effects of single or combined changes in future climate and emissions on global and regional air quality, using both global and regional chemical transport models (CTMs; Weaver et al., 2009; Jacob and Winner, 2009; Fiore et al., 2012). Climate change is likely to decrease background O_3 over remote places due to the elevated humidity and increase O_3 over urban and polluted areas, in part because of higher temperature. Jacob and Winner (2009) concluded that future climate change could increase summertime O_3 by 1–10 ppb over polluted regions in the US in scenarios from the Special Report on Emission Scenarios (SRES; Nakicenovic and Swart, 2000). In one study, climate change in 2050 under the SRES A1B scenario is projected to increase summertime O_3 by 2–5 ppb over large areas in the US, comparable to the effect of reduced anthropogenic emissions of O_3 precursors which reduces O_3 by 2–15 ppb, especially in the east (Wu et al., 2008). The overall effect of climate change on PM is less clear, as different components of PM may respond differently to changes in climate variables (Jacob and Winner, 2009; Tai et al., 2010; Fiore et al., 2012, 2015).

Many studies have also estimated the co-benefits of regional or local GHG mitigation for air quality and human health through reductions in co-emitted air pollutants. Cifuentes et al. (2001) found that GHG mitigation through reduced fossil fuel combustion could bring significant local air-pollution-related health benefits to some megacities. These health benefits have been estimated in many studies (Bell et al., 2008) and give co-benefits ranging from \$2–196 $\mathrm{t\,CO_2^{-1}}$ when monetized, comparable to the costs of GHG reductions (Nemet et al., 2010). A few studies also analyze the co-benefits for future air quality and human health from future regional GHG mitigation scenarios (Thompson et al., 2014; Trail et al., 2015). Thompson et al. (2014) studied the co-benefits of different US climate policies for 2030 domestic air quality and found that when monetized, the human health benefits due to the improved air quality can offset 26–1050 % of the cost of the carbon polices, depending on the policy.

These co-benefit studies may underestimate the total co-benefits as they only consider local or regional climate policies, neglecting benefits outside of the region considered and benefits within those regions from global GHG mitigation. The total co-benefits of global mitigation are relevant as meaningful GHG mitigation requires participation from at least several of the most highly emitting nations. We examined the co-benefits of global GHG reductions for both global and regional air quality and human health, using a global atmospheric model (Model for OZone And Related chemical Tracers, version 4, MOZART-4, hereafter referred to as MZ4) and self-consistent future scenarios (West et al., 2013, referenced hereafter as WEST2013). In addition to evaluating co-benefits through reductions in co-emitted air pollutants, WEST2013 was the first study to quantify co-benefits through a second mechanism: slowing climate change and its effects on air quality. There are several other innovations of WEST2013: we account for global air pollution transport and long-term influences of methane using the global CTM; we consider realistic scenarios in which air pollutant emissions, demographics and economic valuation are modeled consistently; and we evaluate chronic mortality influences of fine PM ($PM_{2.5}$, PM with diameter smaller than 2.5 μm) as well as O_3. WEST2013 concluded that global GHG mitigation could bring significant air quality improvement for both $PM_{2.5}$ and O_3 and avoid 2.2 ± 0.8 million premature deaths globally by 2100 due to the improved air quality. When monetized, the global average marginal co-benefits of avoided mortality were \$50–380 $\mathrm{t\,CO_2^{-1}}$, higher than the previous estimates (Nemet et al., 2010). The co-benefits from the first mechanism of reduced co-emitted air pollutants were shown to be much greater than the co-benefits from the second mechanism via slowing climate change.

The WEST2013 study is limited by the coarse resolution of the CTM used ($2^\circ \times 2.5^\circ$ horizontally). Here we investigate the co-benefits of global GHG mitigation for US air quality at much finer resolution (36 km × 36 km), building on the scenarios in the global study. WEST2013 simulated co-benefits in 2030, 2050 and 2100, and we choose here to downscale the results in 2050, as climate change influences air quality by 2050, and it is within the time frame of current decision making for both climate change and air quality. We use a comprehensive modeling framework in the downscaling process, including a regional climate model to dynamically downscale the global climate to the contiguous United States (CONUS), an emissions processing program to directly process the global anthropogenic emissions to the regional scale, and we create dynamical boundary conditions (BCs) from the global co-benefit outputs for the regional CTM. We quantify the total co-benefits of global GHG mitigation for US air quality for both $PM_{2.5}$ and O_3 and then separate the co-benefits from the two mechanisms analyzed by WEST2013. We also quantify the co-benefits from domestic GHG mitigation vs. the co-benefits from those of foreign countries' reductions. We then present the co-benefits from global and domestic GHG mitigation for nine US regions.

With regard to previous studies on the effect of climate change on future air quality (e.g., Jacob and Winner, 2009), our work differs in our reframing of this impact as a co-

benefit of slowing climate change from GHG mitigation and by analyzing that co-benefit through realistic future scenarios, following WEST2013. With regard to previous co-benefits studies that have been conducted on a regional scale (e.g., Thompson et al., 2014), this research differs by embedding the regional co-benefits study in a consistent global context, accounting for the effects of changes in global air pollutant emissions and climate change on US air quality.

2 Methodology

Future air quality changes under global and regional GHG mitigation scenarios are simulated using a regional CTM. The scenarios modeled here are built on those of WEST2013, who compared the Representative Concentration Pathway 4.5 (RCP4.5) scenario with its associated reference scenario (REF). Air pollutant emissions in REF are state-of-the-art long-term emissions projections created by using the Global Change Assessment Model (GCAM; Thomson et al., 2011). RCP4.5 was developed based on REF by applying a global carbon price to all world regions and all sectors including carbon in terrestrial systems. As discussed by van Vuuren et al. (2011), the air pollutant emissions for the four RCP scenarios were prepared by different groups using different models and assumptions, so they are inconsistent with one another. But by comparing REF with RCP4.5, we use a self-consistent pair of scenarios, where the difference is uniquely attributed to a climate policy. WEST2013 used both emissions and meteorology from RCP4.5 to simulate future air quality under the RCP4.5 climate policy and used emissions from REF and meteorology from RCP8.5 to simulate future air quality assuming no climate policy. Since no general circulation model (GCM) conducted future climate simulations for the REF scenario, RCP8.5 is used as a proxy for the future climate under REF. The differences between these two scenarios give the total co-benefits for future air quality under climate policy from RCP4.5. Through one extra simulation with emissions from RCP4.5 together with RCP8.5 meteorology (e45m85 in Table 1) and by comparing with REF and RCP4.5, WEST2013 separated the total co-benefits into the two mechanisms: the co-benefits from reductions in co-emitted air pollutants and co-benefits from slowing climate change and its influence on air quality.

Here we conduct downscaling processes to provide fine-resolution inputs for the regional CTM. We use the Weather Research and Forecasting model version 3.4.1 (WRF; Skamarock and Klemp, 2008) to downscale the future global climate from the GCM to the regional scale at a horizontal resolution of 36×36 km for the CONUS. We directly process global anthropogenic emissions to regional scale using the Sparse Matrix Operator Kernel Emissions (SMOKE, v3.5, Houyoux et al., 2000) program. The outputs from the global MZ4 simulations of WEST2013 (Table 1) are downscaled to provide initial conditions (ICs) and dynamic hourly BCs for the regional CTM. The latest version of the Community Multi-scale Air Quality model (CMAQ, v5.0.1; Byun and Schere, 2006) is used as the regional CTM to simulate air quality changes over the CONUS domain. WEST2013 simulated 5 consecutive years for each scenario and used the last 4 years' average for the data analysis with the first year as a spin-up. Due to the limitations of computational resources, we run CMAQ for 40 months consecutively for each scenario, with the first 4 months as spin-up, and analyze the results as 3-year averages.

2.1 Regional meteorology

WEST2013 used NOAA Geophysical Fluid Dynamics Laboratory (GFDL) atmospheric model AM3 (Donner et al., 2011; Naik et al., 2013) simulations to provide global meteorology for MZ4. Here we dynamically downscale GFDL AM3, which has a horizontal resolution of $2^\circ \times 2.5^\circ$, to 36×36 km over the CONUS using the WRF model. GFDL AM3 meteorology for the two RCP scenarios (RCP8.5 and RCP4.5) in 2050 used by WEST2013 is downscaled using a one-way nesting configuration for 5 consecutive years. WRF is initialized at 00:00 Coordinated Universal Time (UTC) 1 January 2048 and run for a 12-month spin-up, then run continuously through 00:00 UTC 1 January 2053. A historical period from GFDL AM3 is also downscaled with WRF initialized at 00:00 UTC 1 January 1999 and run for a 12-month spin-up, then run continuously through 00:00 UTC 1 January 2004. The WRF physics options include the rapid radiative transfer model for global climate models (Iacono et al., 2008) for longwave and shortwave radiation, WRF single-moment six-class microphysics scheme (Hong and Lim, 2006), the Grell ensemble convective parameterization scheme (Grell and Devenyi, 2002), the Yonsei University planetary boundary layer scheme (Hong et al., 2006) and the Noah land surface model (Chen and Dudhia, 2001). The WRF configuration also applies spectral nudging. Otte et al. (2012) and Bowden et al. (2012, 2013) demonstrated that using nudging in WRF improves the overall accuracy of the simulated climate over the CONUS at 36 km and does not squelch extremes in temperature and precipitation. In particular, spectral nudging affects the model solution through a nonphysical term in the prognostic equations based on the difference between the spectral decomposition of the model solution and the reference analysis. Spectral nudging is used to constrain WRF toward synoptic-scale wavelengths resolved by GFDL AM3 exceeding 1200 km. Nudging is applied equally to potential temperature, wind and geopotential with a nudging coefficient of 1.0×10^{-4}, which is equivalent to a timescale of 2.8 h. The downscaled meteorology from WRF is used to provide meteorological inputs to CMAQ. Hourly WRF outputs are processed using the Meteorology-Chemistry Interface Processor (MCIP v4.1; Otte and Pleim, 2010) to provide meteorological inputs for CMAQ.

Table 1. List of CMAQv5.0.1 simulations in this study. Hourly BCs are from the MOZART-4 (MZ4) simulations of WEST2013. We fix the methane (CH_4) background concentrations in CMAQ consistent with the RCP scenarios and WEST2013.

Years	Scenario	Emissions	Meteorology	BCs	CH_4
2000	S_2000	2000	2000	MZ4 2000	1766 ppbv
2050	S_REF	REF	RCP8.5	MZ4 REF	2267 ppbv
	S_RCP45	RCP4.5	RCP4.5	MZ4 RCP4.5	1833 ppbv
	S_Emis	RCP4.5	RCP8.5	MZ4 e45m85[b]	1833 ppbv
	S_Dom	RCP4.5 for US, REF for Can, Mex[a]	RCP8.5	MZ4 REF	2267 ppbv

[a] The part of Canada and Mexico in the domain. [b] Global simulation using RCP4.5 emissions together with RCP8.5 meteorology in 2050.

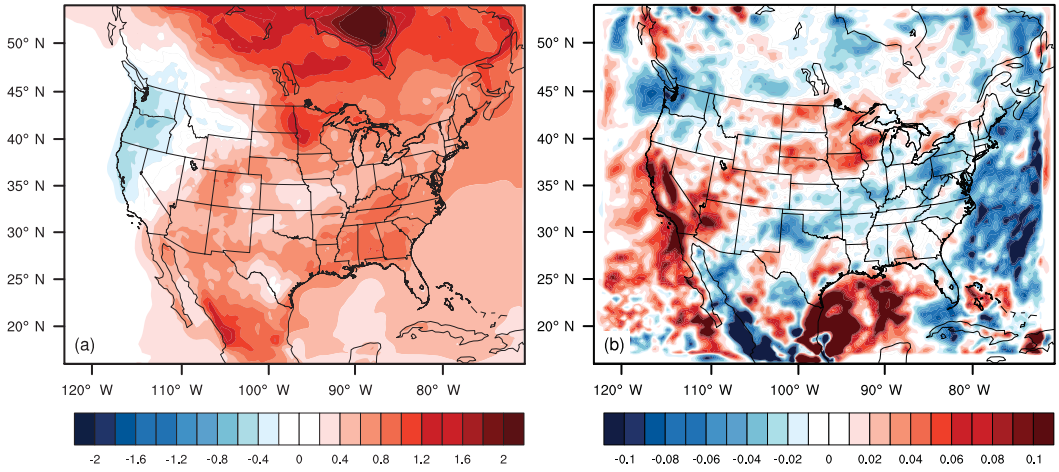

Figure 1. Changes in **(a)** 2 m temperature (°C) and **(b)** precipitation (mm day^{-1}) centered on 2050 between RCP8.5 and RCP4.5 (RCP8.5–RCP4.5).

We compare the downscaled WRF and the global GFDL AM3 simulations (for 3-year averages instead of 4 to be consistent with CMAQ outputs below), for 2 m temperature (T2) with 21 years (1979 to 2000) of observation data from the 32 km North America Regional Reanalysis (NARR; Mesinger et al., 2006) and for precipitation with 41 years (1948 to 1998) of observation data from the 0.25° × 0.25° Unified US precipitation data product from the NOAA Climate Prediction Center (Higgins et al., 2000). The large-scale spatial patterns for both T2 and precipitation between WRF and GFDL AM3 are similar (Fig. S1 in the Supplement). However, the downscaled simulations help resolve important features that influence the average regional climate, such as those related to topography. Comparing WRF future projected change centered on 2050 with 2000, we see that the 3-year average of T2 generally increases over the entire US for both RCP8.5 and RCP4.5 (Figs. S2–S3). Temperature increases are largest for extreme northeastern latitudes, the southeast and southwest US in both scenarios, with a US average warming of 3.05 and 2.59 °C for RCP8.5 and RCP4.5, respectively. Additionally, precipitation is projected to decrease over most of the US in both scenarios with a US average decrease of 0.20 and 0.15 mm day^{-1} in RCP8.5 and RCP4.5. Comparing the changes between scenarios (RCP8.5 minus RCP4.5), Fig. 1 illustrates that temperature increases are smaller in RCP4.5 throughout the CONUS, except in the northwest. The precipitation difference between scenarios has a larger spatial variability than the T2. Ignoring other influences of climate change, decreases in precipitation would be expected to decrease PM wet scavenging and increase PM concentration.

2.2 Regional emissions

Similar studies in the past have typically chosen to run SMOKE with the present-day US National Emission Inventory (NEI) and then scale the SMOKE outputs into future years, using the mass ratio of projected future to present-day emissions from global inventories (e.g., Hogrefe et al., 2004; Nolte et al., 2008; Avise et al., 2009; Chen et al., 2009; Gao et al., 2013). By doing this, the traditional method assumes that future spatial distributions of emissions stay the same as the current NEI. Instead, we use SMOKE to directly process the

Table 2. Anthropogenic emissions in the US for major air pollutants in 2000 and 2050 from REF and RCP4.5 ($Tg\,yr^{-1}$) and the relative differences (Relative diff) between RCP4.5 and REF in 2050 ((RCP4.5 – REF)/REF × 100).

	2000	2050 REF	2050 RCP4.5	Relative diff (%)
SO_2	14.84	2.46	1.75	−28.78
NH_3	3.34	4.56	4.30	−5.56
NO_x	19.57	4.40	3.92	−10.93
CO	92.74	11.42	11.25	−1.48
NMVOC	15.23	8.07	7.16	−11.21
EC	0.42	0.22	0.21	−7.59
OC	0.71	0.35	0.33	−6.17
$PM_{2.5}$[1]	4.14	1.87	1.57	−15.80
PMC[2]	11.02	5.50	4.63	−15.80

[1,2] $PM_{2.5}$ and PMC are the total emissions back-calculated based on the EC and OC.

global emissions in 2000 and in 2050 from REF and RCP4.5 to provide temporally and spatially resolved CMAQ emission input files. We first regrid the global emissions datasets at 0.5° × 0.5° with finer resolution (36 km × 36 km) and then apply source-specific temporal and speciation profiles from the NEI to assign temporal variations and re-speciate the PM and volatile organic compound (VOC) species. By regridding the REF and RCP4.5 data, we account better for changes in the spatial distribution changes in future emissions projected in the RCPs (Figs. S4–S10) but do not provide additional spatial detail beyond what is provided by the RCPs at 0.5° resolution, whereas the traditional method only considers changes in the magnitude of air pollutants in the future, assuming a constant spatial and sectoral distribution. We use constant (year 2000) land use and land cover for all simulations in WRF and CMAQ, whereas the spatial distributions of anthropogenic emissions change in the RCP scenarios.

In addition, the RCP datasets report only elemental carbon (EC) and organic carbon (OC) but ignore emissions of other primary PM species. Here we back-calculate the total $PM_{2.5}$ and PM coarse (PMC) primary emissions for all sectors from the reported EC and OC. We first derive the emission fractions of EC and OC in each sector by cross-comparing the definitions of the sectors in IPCC, the Source Clarification Codes (SCC) in the speciation cross-reference file (http://www.airqualitymodeling.org/cmaqwiki/index.php?title=CMAQv5.0_GSREF_example) and the NEI PM speciation profile file (http://www.airqualitymodeling.org/cmaqwiki/index.php?titleCMAQv5.0_GSPRO_Example, Table S1 in the Supplement). In back-calculating total PM emissions from BC and OC, there is usually more than one subcategory within one sector; e.g., the sector "Industries" includes emissions from the subcategory of "1A2_2A_B_C_D_E" (Table S1). When that happens, we use the speciation cross-reference file from the subcategory with the largest mass fraction in this sector, following the methods of Reff et al. (2009) and Xing et al. (2013). Then we calculate the total $PM_{2.5}$ and PMC in each grid cell by dividing the reported EC and OC by their emission fractions individually and average these two. By doing this, we increase the total $PM_{2.5}$ emissions of the RCPs by incorporating the inorganic components of primary PM, such as sulfate and nitrate. We check these results by comparing the total 2000 $PM_{2.5}$ emissions of $4.14\,Tg\,yr^{-1}$ in this study (Table 2) with other studies, finding that it is comparable to the total of $4.69\,Tg\,yr^{-1}$ in 2001 from the US NEI (http://www.epa.gov/ttnchie1/trends/). Our calculated $PM_{2.5}$ emission is also lower than the estimated $5.53\,Tg\,yr^{-1}$ in 2000 by Xing et al. (2013), which used an activity data-based approach to develop consistent temporally resolved emissions from 1999 to 2010.

In Table 2, we list the US anthropogenic emissions for major air pollutants in 2000 and 2050 from REF and RCP4.5. Significant decreases are seen for most pollutants from 2000 to 2050 for both REF and RCP4.5, except for NH_3 which is projected to increase due to agricultural activity (van Vuuren et al., 2011). Comparing RCP4.5 and REF, emissions of $PM_{2.5}$ and O_3 precursors also decrease, including EC (7.59 %) and OC (6.17 %), with NO_x and non-methane volatile organic compounds (NMVOCs) decreasing by more than 10 %. SO_2 has the largest relative decreases between RCP4.5 and REF in 2050 (28.78 %). Large spatial variations in emissions reductions are also seen over the US, with the largest reductions seen in the east and west urban areas of US for most air pollutants and smaller reductions in the Great Plains (Figs. S4–S10).

Biogenic emissions are estimated using the Biogenic Emission Inventory System (BEIS v3.14), which responds to the changing climate for different scenarios. It is configured to run online in CMAQ and calculates the emissions of 35 chemical species, including 14 monoterpenes and 1 sesquiterpene. We assume that land use and land cover will stay constant in the future for the purpose of estimating biogenic emissions. We also use the BEIS online calculation for natural soil NO_x emissions. The online option of lightning is also turned on to calculate the NO_x emissions by estimating the number of lightning flashes based on the modeled convective precipitation, which also changes with climate. We prepare the ocean–land mask for the domain to calculate sea salt emissions, which can be significant in coastal environments (Kelly et al., 2010).

2.3 Regional air quality model and dynamical chemical BCs

The latest CMAQ model (https://www.cmascenter.org/cmaq/index.cfm) is used to perform the regional air quality simulations with the CB05 chemical mechanism and updated toluene reactions. The model incorporates the newest aerosol module (AE6), including features of new PM speciation

(Reff et al., 2009), oxidative aging of primary organic carbon (Simon and Bhave, 2012), and an updated treatment and tracking of crustal species (e.g., Ca^2+, K^+, Mg^{2+}) and trace metals (e.g., Fe, Mn; Fountoukis and Nenes, 2007). Several other enhancements in v5.0 of CMAQ were discussed by Appel et al. (2013) and Nolte et al. (2015), and there are no significant changes for the aerosol module between v5.0 and v5.0.1 (http://www.airqualitymodeling.org/cmaqwiki/index.php?titleCMAQ_version_5.0.128July_2012_release29_Technical_Documentation). The model is configured with 34 vertical layers, with the lowest level being 34 m high, to the highest level at 50 hPa. The horizontal resolution is 36 km by 36 km for the CONUS domain. $PM_{2.5}$ is calculated from the CMAQ output as the sum of the species EC, OC, secondary organic aerosol (SOA), non-carbon organic matter (NCOM), nitrate (NO_3^-), sulfate (SO_4^{2-}), ammonium (NH_4^+), sodium (Na^+), chloride (Cl^-), eight crustal and trace metal species, and other unspeciated fine PM (OTHER).

The dynamical BCs for this study are provided by the global MZ4 simulations of WEST2013. The hourly boundary values from MZ4 are horizontally interpolated from coarser resolution to the regional finer resolution and also vertically interpolated as MZ4 and CMAQ have different vertical layers. Chemical species are mapped between MZ4 and CMAQ v5.0.1, due to the different chemical mechanisms used by these two models, following the descriptions of Emmons et al. (2010) and ENVIRON (http://www.camx.com/download/support-software.aspx). For the chemical species in CMAQ that do not exist in MZ4, values are set to defaults as suggested by the CMAQ website.

2.4 Scenarios

We simulate scenarios in CMAQ comparable to WEST2013, except that we carry out one extra scenario to quantify the co-benefits from domestic vs. foreign GHG mitigation (Table 1). S_2000 is conducted to evaluate CMAQ model performance and to compare it with future scenarios. For this study, we run four scenarios in 2050. The differences between S_RCP45 and S_REF are the total co-benefits for US air quality from global GHG mitigation. The emission benefit from the first mechanism is calculated as the difference between S_ Emis and S_REF, for which the change in methane concentration is included as an emission benefit and the meteorology benefit is calculated as S_RCP45 minus S_Emis. By comparing S_Dom (applying GHG mitigation from RCP4.5 scenario in the US only) with S_REF and S_RCP45 with S_Dom, we quantify the co-benefits from domestic and foreign GHG mitigation. The co-benefits from foreign reductions are found by simple subtraction (S_RCP45 – S_REF) – (S_Dom – S_REF) = S_RCP45 – S_Dom. In estimating the co-benefits of domestic reductions, we account for the influences of methane and of global climate change as foreign influences (as most methane and GHG emissions are outside of the US) and assume that US air pollutant emissions have small effects on global or regional climate, such as through aerosol forcing. In each scenario, we fix global methane at concentrations given by the RCPs (Table 1) and account for methane changes as a foreign influence, neglecting the fraction of global anthropogenic methane emissions that are from the US (7.4 % in 2050 REF scenario and 7.0 % in 2050 RCP4.5). All scenarios are set up as continuous runs, with S_2000 running from September 2000 to December 2003, with the first 4 months in 2000 as spin-up. The future scenarios are run from September 2049 to December 2052 with the months in 2049 as spin-up. Results are presented as the average of 3 years.

3 Results

3.1 CMAQ model evaluation

The CMAQ model has been broadly used to study regional future air quality (Hogrefe et al., 2004; Tagaris et al., 2007; Nolte et al., 2008; Lam et al., 2011; Gao et al., 2013) and has been evaluated in many applications (Appel et al., 2010, 2011, 2013; Nolte et al., 2015). Here we evaluate the CMAQ v5.0.1 performance by comparing the model outputs from S_2000 with observations in 2000 from the Interagency Monitoring of PROtected Visual Environments (IMPROVE; http://vista.cira.colostate.edu/improve/), the Chemical Speciation Network (CSN; previously known as STN, http://www.epa.gov/ttn/amtic/speciepg.html), the Clean Air Status and Trends Network (CASTNET; http://epa.gov/castnet/javaweb/index.html) for total $PM_{2.5}$ and its components, and the EPA Air Quality System (AQS; http://www.epa.gov/ttn/airs/airsaqs/detaildata/downloadaqsdata.htm) for O_3. We pair the model outputs with observations in space and time and calculate four groups of statistics to evaluate model performance: median bias (MdnB, $\mu g\,m^{-3}$ for $PM_{2.5}$ and ppb for O_3), normalized median bias (NMdnB, %), median error (MdnE, $\mu g\,m^{-3}$ and ppb) and normalized median error (NMdnE, %, Supplement). Median metrics are used here instead of the mean, as for data with non-normal distributions (i.e., PM species) the median gives a better representation of the central tendency of the data (Appel et al., 2008). For O_3 evaluation, we use both the maximum daily 1 h (1 h_O_3) and maximum daily 8 h average (MDA8) and also calculate these metrics with a cutoff value of 40 ppb for the observed O_3 to evaluate the model's reliability in predicting ozone values relevant for the national ambient air quality standards (NAAQS; USEPA, 2007). Model performance is not expected to be perfect as meteorology does not correspond with actual year 2000 meteorology and emissions are derived from global datasets rather than the specific NEI year dataset for the US

For total $PM_{2.5}$, overall model performance is good and the NMdnE for IMPROVE and CSN are less than 50 %, with

Table 3. Evaluation of the S_2000 simulation (average of 3 years modeled) with surface observations in 2000 for $PM_{2.5}$ ($\mu g\,m^{-3}$) and O_3 (ppb).

	Pollutants	MdnB	NMdnB (%)	MdnE	NMdnE (%)
IMPROVE	$PM_{2.5}$	−0.89	−23.31	1.88	49.46
CSN	$PM_{2.5}$	−2.85	−27.44	4.29	41.30
AQS	1 h_O_3	8.97	18.40	13.25	27.60
AQS	1 h_O_3_40*	2.79	4.76	9.89	17.36
AQS	MDA8_O_3	11.87	28.01	14.13	33.35
AQS	MDA8_O_3_40*	3.95	7.37	9.09	16.95

* 1 h_O_3_40 and MDA8_O_3_40: observations below 40 ppb are excluded from the comparison.

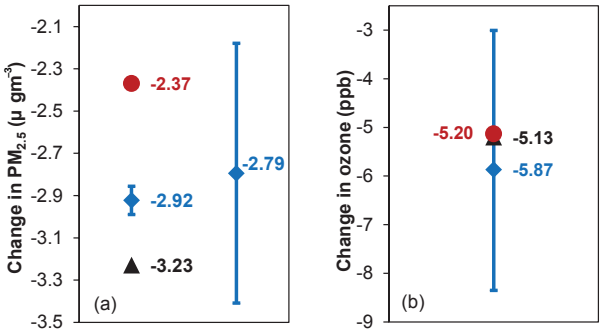

Figure 2. Comparison of annual US average concentration changes for RCP4.5 in 2050 relative to 2000, for this study (black triangle), MZ4 from WEST2013 (red circle), and the ensemble mean (blue diamond) and multi-model range from ACCMIP (blue lines), for **(a)** $PM_{2.5}$ and **(b)** O_3. In panel **(a)**, the total $PM_{2.5}$ reported by the ACCMIP models is shown on the left and the $PM_{2.5}$ estimated as a sum of species $BC + OA + SOA + SO_4 + NO_3 + NH_4 + 0.25 \times SeaSalt + 0.1 \times Dust$ following Fiore et al. (2012) and Silva et al. (2013) shown on the right. Values shown are the average of 3 years for CMAQ and MZ4 and 5 to 10 years for ACCMIP for three models (LMDzORINCA, GFDL-AM3 and GISS-E2-R) that report O_3 and two models (GFDL-AM3 and GISS-E2-R) that report $PM_{2.5}$.

slight differences in performance (Table 3). CMAQ underestimates $PM_{2.5}$ in these two networks and also its components in all three networks (Table S2), except that it overestimates SO_4^{2-} compared with IMPROVE and NH_4^+ with CSN. Compared with other components, OC and EC are not well predicted, with higher NMdnB: −63.55 and −37.00 % in IMPROVE (OC and EC are not measured in the other two networks). In simulating $PM_{2.5}$ and its species, model performance is better in winter than in summer (not shown here). The model overestimates surface O_3 as indicated by the positive MdnB (ppb) and NMdnB (%). The NMdnE for the 1 h O_3 (MDA8-O_3) declines from 27.60 (33.35 %) to 17.36 % (16.95 %) after we apply the cutoff value of 40 ppb. The overprediction is slightly lower for 1 h_O3 than for MDA8-O_3; however, this difference becomes smaller when we consider the cutoff values. By comparing the simulated annual $PM_{2.5}$ and O_3 in 2000 (both are 3-year averages) between MZ4 and CMAQ, we see that CMAQ captures urban-scale air quality better than MZ4 (Fig. S11).

3.2 Air quality changes in 2050

Here we show the seasonal and spatial patterns of future air quality changes centered in 2050 relative to 2000 from REF and RCP4.5 (Figs. S12 to S15). The 3-year seasonal average of $PM_{2.5}$ over the entire US decreases in 2050 in both S_REF and S_RCP45 compared with S_2000, especially in the eastern US and California (CA). The seasonal decreases are largest in winter, with US averages in S_REF (S_RCP45) of 4.42 (4.88) $\mu g\,m^{-3}$, and lowest in the summer of 1.55 (2.00) $\mu g\,m^{-3}$, with annual average of 2.76 (3.23) $\mu g\,m^{-3}$. The 3-year seasonal average of O_3 decrease significantly in summer on both the east and west coast, with a US average of 6.31 (9.50) ppb in S_REF (S_RCP45). O_3 increases over the northeast and west US in winter in both S_REF and S_RCP45, caused by the weakened NO titration as a result of the large NO decrease in the two scenarios (Table 2), as also reported by other studies (Gao et al., 2013; Fiore et al., 2015), and the large methane increases in the RCP8.5 scenario (Gao et al., 2013). The magnitude of the decreases between S_REF and S_2000 is lower than that between S_RCP45 and S_2000, as the REF scenario did not apply a GHG mitigation policy and thus has less emission reductions.

We then compare these air quality changes in 2050 with the MZ4 simulations of WEST2013 for both S_REF (Fig. S16) and S_RCP45 (Fig. 2) and for S_RCP45 with the ensemble model means from the Atmospheric Chemistry and Climate Model Intercomparison Project (ACCMIP; Lamarque et al., 2013) following Fiore et al. (2012), as no ACCMIP models simulated REF in 2050. For the US annual average $PM_{2.5}$, the decrease in 2050 for S_RCP45 relative to 2000 in this study (3.23 $\mu g\,m^{-3}$) is modestly higher than both the results from MZ4 and the ACCMIP ensemble mean but within the range of ACCMIP models when $PM_{2.5}$ is calculated as a sum of species. The future O_3 changes in our study (5.20 ppb) are clearly in the range of ACCMIP results and nearly identical to MZ4 (5.13 ppb). Comparisons of the air quality changes in 2050 for S_REF relative to 2000 between CMAQ and MZ4 are similar, except that the magnitudes of the changes are smaller than those for S_RCP45 (Fig. S16). CMAQ better simulates air quality changes in urban environments on a finer scale compared with MZ4.

3.3 Total co-benefits for US air quality from global GHG mitigation

Projected 3-year average $PM_{2.5}$ concentrations in 2050 in both scenarios (S_REF and S_RCP45) are higher in the eastern US and the west coast of CA and lower in the western US (Fig. 3). The total co-benefits for US air quality

(S_RCP45 minus S_REF) show notable decreases in major air pollutants in 2050. The total co-benefits for $PM_{2.5}$ over the US show a significant spatial gradient over the US domain, which is greatest in the eastern US, especially urban areas, as well as CA, ranging from 0.4 to 1.0 $\mu g\,m^{-3}$, and least in the Rocky Mountains and northwest, with values below 0.4 $\mu g\,m^{-3}$. The total co-benefits for $PM_{2.5}$ averaged over the US are 0.47 $\mu g\,m^{-3}$, with the largest contribution from organic matter (OM, including primary OC, SOA and NCOM), accounting for 45 % of the total (0.21 $\mu g\,m^{-3}$), followed by sulfate (0.11 $\mu g\,m^{-3}$) and ammonia (0.05 $\mu g\,m^{-3}$; Fig. S17). The total co-benefits are highest in fall, with a US domain average of 0.55 $\mu g\,m^{-3}$, and lowest in spring (0.41 $\mu g\,m^{-3}$; Fig. 4). Notice that the region with greatest co-benefits shifts from central areas in winter and spring to the east in summer and fall, with the largest component of OM also shifting from primary OC to SOA (Fig. S18).

Future O_3 is presented here as the ozone season average (from May to October) of MDA8. In general, 2050 O_3 concentrations in S_REF and S_RCP45 are projected to be high in the southern US, especially over the coastal areas and higher in the west than the east (Fig. 5). The total co-benefits for O_3 are fairly uniformly significant over the entire US domain, but slightly higher in the northeast and northwest and range from 2–5 ppb with a domain average of 3.55 ppb, unlike $PM_{2.5}$, which is higher over urban regions. The uniformity of the total O_3 co-benefits suggests that they are strongly influenced by global O_3 reductions.

The total co-benefit for $PM_{2.5}$ from this study (0.47 $\mu g\,m^{-3}$ over US) is lower than WEST2013 (area-weighted 3-year averages of 0.72 $\mu g\,m^{-3}$ over the US), especially over the northwest and center of the US (Fig. S20). Analyzing the components of $PM_{2.5}$, we find that this difference is mainly caused by OM, with a US annual average of 0.40 $\mu g\,m^{-3}$ in WEST2013 and 0.21 $\mu g\,m^{-3}$ in this study (Fig. S21). For other components (EC, SO_4^{2-}, NO_3^- as reported in MZ4 of WEST2013), the CMAQ results are slightly lower than WEST2013 but share a similar spatial pattern (Figs. S22–S25). We expect that the total co-benefits of $PM_{2.5}$ in this study might be higher than WEST2013, as we account for inorganic primary PM emissions in SMOKE. A possible explanation may be that different chemical mechanisms and deposition processes are adopted for organic aerosols in MZ4 and CMAQ, which may lead to a shorter atmospheric lifetime for PM in CMAQ than in MZ4. The differences in the meteorology (e.g., the precipitation and temperature) between the downscaled WRF and the GFDL could also contribute to this difference. Total co-benefit of O_3 from this study (3.55 ppb over US) is comparable to WEST2013 (3.71 ppb) in both the magnitude and spatial distribution (Fig. S25).

3.4 Co-benefits from the two mechanisms

We quantify the co-benefits of global GHG mitigation for $PM_{2.5}$ and O_3 through two mechanisms: reduced co-emitted air pollutants (S_Emis–S_REF) and slowing climate change and its effect on air quality (S_RCP45–S_Emis). The reduction in co-emitted air pollutants has a much greater effect than slowing climate change for $PM_{2.5}$, accounting for 96 % of the US average $PM_{2.5}$ decrease. The emission benefit for $PM_{2.5}$ over the US domain is 0.45 $\mu g\,m^{-3}$ and greatest near urban areas where emissions are reduced (Fig. 6), with the largest contribution from OM (0.172 $\mu g\,m^{-3}$ over the US), followed by sulfate (0.107 $\mu g\,m^{-3}$) and ammonia (0.048 $\mu g\,m^{-3}$). In Fig. S18, the OM decrease is caused mainly by primary organic carbon (POC, 0.074 $\mu g\,m^{-3}$ decreases), followed by biogenic SOA (ORGB, 0.057 $\mu g\,m^{-3}$) and non-carbon organic matter (NCOM, 0.048 $\mu g\,m^{-3}$). The POC and NCOM decreases are caused mainly by emission reductions, while the SOA decrease is caused mainly by changing climate (Fig. S19). Slowing climate change only accounts for 4 % of the US average total $PM_{2.5}$ decreases (0.02 $\mu g\,m^{-3}$). It also has different signs of effect over the US, reducing $PM_{2.5}$ in the southern US but increasing in the north.

For O_3, the emission benefit is also larger than the climate benefit, accounting for 89 % of the total O_3 decreases averaged over the US. The emission benefit for O_3 over the US domain is 3.16 ppb and much more uniform over the US, but slightly higher over the northeast and northwest. Slowing climate change accounts for 0.39 ppb O_3 decreases – 11 % of the total and mainly in the Great Plains and the east, where temperatures are cooler under RCP4.5 compared with RCP8.5 (Fig. 1). The dominance of the emission co-benefit over the climate co-benefit for both $PM_{2.5}$ and O_3 is consistent with WEST2013.

3.5 Co-benefits from domestic and foreign GHG mitigation

We also investigate the co-benefits from domestic GHG mitigation by comparing S_Dom with S_REF, on the one hand, versus foreign GHG reductions by comparing S_RCP45 with S_Dom (Fig. 7), on the other hand. For $PM_{2.5}$, domestic GHG mitigation accounts for 74 % (0.35 $\mu g\,m^{-3}$) of the total $PM_{2.5}$ decrease over the whole US, with the greatest effect over the east and CA, where emissions of $PM_{2.5}$ and its precursors are greatly reduced (Figs. S3–S9). The benefits from foreign GHG reductions for the US $PM_{2.5}$ change are only obvious in the southern US, influenced by emission reductions in Mexico and global climate change. We conclude that domestic GHG mitigation has a greater influence on US $PM_{2.5}$ than reductions in foreign countries but that foreign reductions also make a noticeable contribution, accounting for 26 % of total $PM_{2.5}$ decreases over the US and a greater fraction (40 %) in the south, southwest and east N central regions.

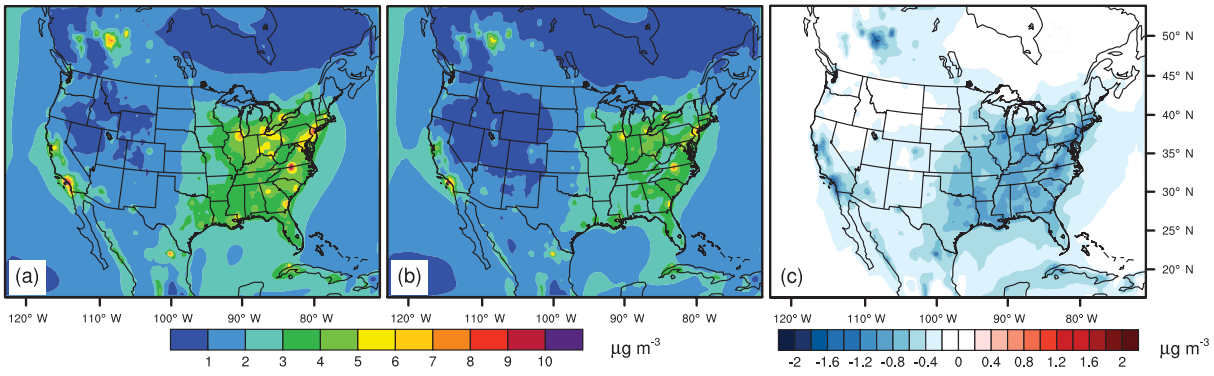

Figure 3. The 3-year average $PM_{2.5}$ ($\mu g\,m^{-3}$) distributions in 2050 from **(a)** S_REF, **(b)** S_RCP45 and **(c)** the total co-benefits (shown as the difference between S_RCP45 and S_REF). Blue colors in panel **(c)** indicate an air quality improvement.

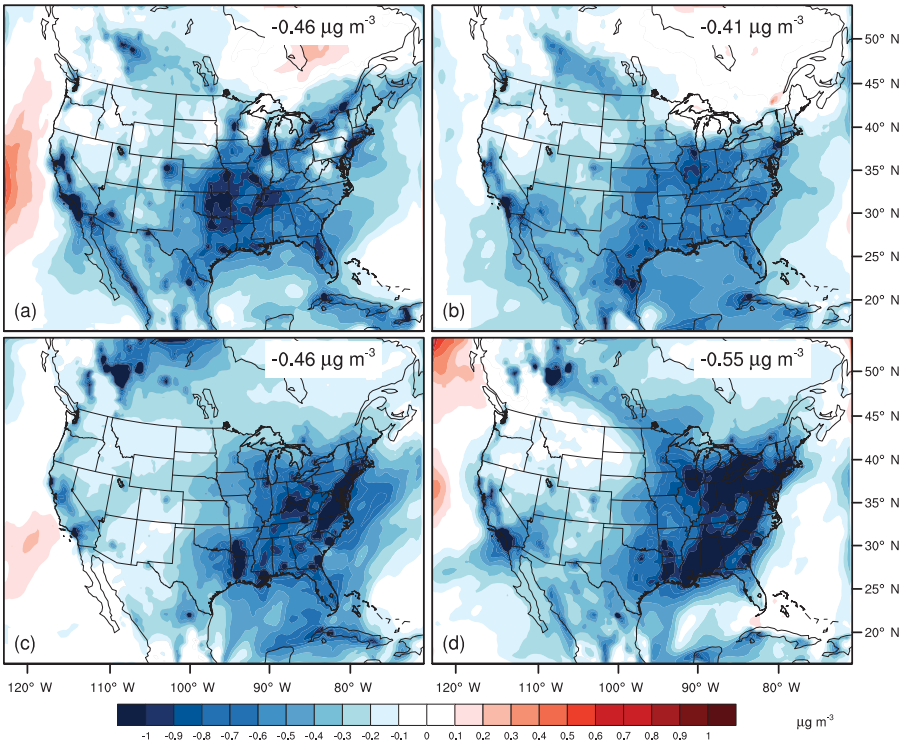

Figure 4. Seasonal distributions of total co-benefits for $PM_{2.5}$ ($\mu g\,m^{-3}$) for **(a)** winter, **(b)** spring, **(c)** summer and **(d)** fall.

Note that the uncertainty in the foreign co-benefits is much larger than for the domestic reductions (Table S3). Longer simulations would be needed to reduce this uncertainty.

For O_3, foreign countries' GHG mitigation has a much larger influence on the US, accounting for 76 % (2.69 ppb) of the total O_3 decrease, compared with 24 % from domestic GHG mitigation (Fig. 7). The US experiences greater O_3 decreases in the north than the south, which is likely influenced in part by the air quality improvement in Western Canada as a result of slowing deforestation due to the climate policy in RCP4.5 (West et al., 2013). This large influence of foreign reductions for O_3 highlights the importance of global methane reductions in RCP4.5 (anthropogenic emissions of 330 Tg yr^{-1} in 2050 in RCP45, compared to 432 Tg yr^{-1} in REF), particularly in Asia, and intercontinental transport.

3.6 Regional co-benefits and variability

We then quantify the co-benefits over nine US climate regions defined by the National Oceanic and Atmospheric Administration (Fig. S26) and their domestic and foreign components. The central, southeast, northeast and south regions have the largest total co-benefits for $PM_{2.5}$ (regional annual means of 0.78, 0.75, 0.62 and 0.62 $\mu g\,m^{-3}$), and the north-

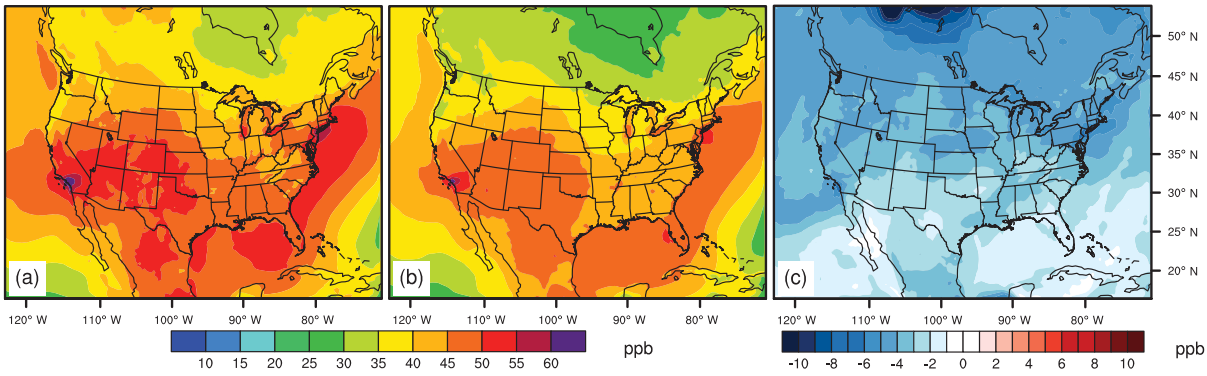

Figure 5. The 3-year ozone season average (May to October) of MDA8 O_3 (ppb) from **(a)** S_REF, **(b)** S_RCP45 and **(c)** the total co-benefits (shown as the difference between S_RCP45 and S_REF). Blue colors in panel **(c)** indicate an air quality improvement.

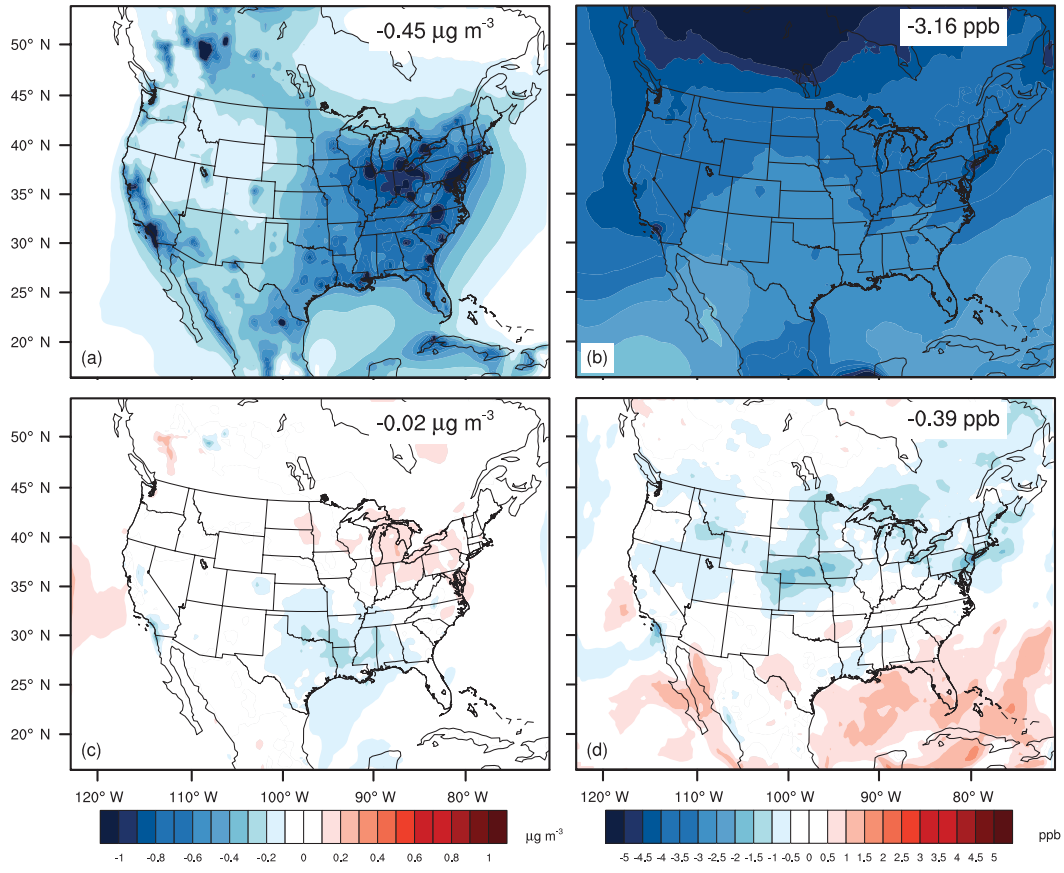

Figure 6. Benefits of reduced co-emitted air pollutants (**a**, **b**; S_Emis–S_REF) vs. slowing climate change (**c**, **d**; S_RCP45–S_Emis) for $PM_{2.5}$ **(a, c)** and ozone season MDA8 surface O_3 **(b, d)**. Blue colors indicate an air quality improvement. The numbers on the plots are the 3-year average of air quality changes over the US.

west has the lowest total co-benefits (0.16 µg m^{-3}; Fig. 8). Domestic GHG mitigation has the largest effect over these same regions and lowest effects over the northwest and west north central areas, with means of 0.13 µg m^{-3}. Foreign co-benefits are greatest over the south, southwest, center and southeast and lowest over the northwest (Table S3). As a fraction of the total co-benefits, the domestic co-benefit is highest in the northeast, east north central and central areas accounting for more than 80 % of the total, while foreign co-benefits are highest over the southwest, south and west north central areas, accounting for about 40 % of the total.

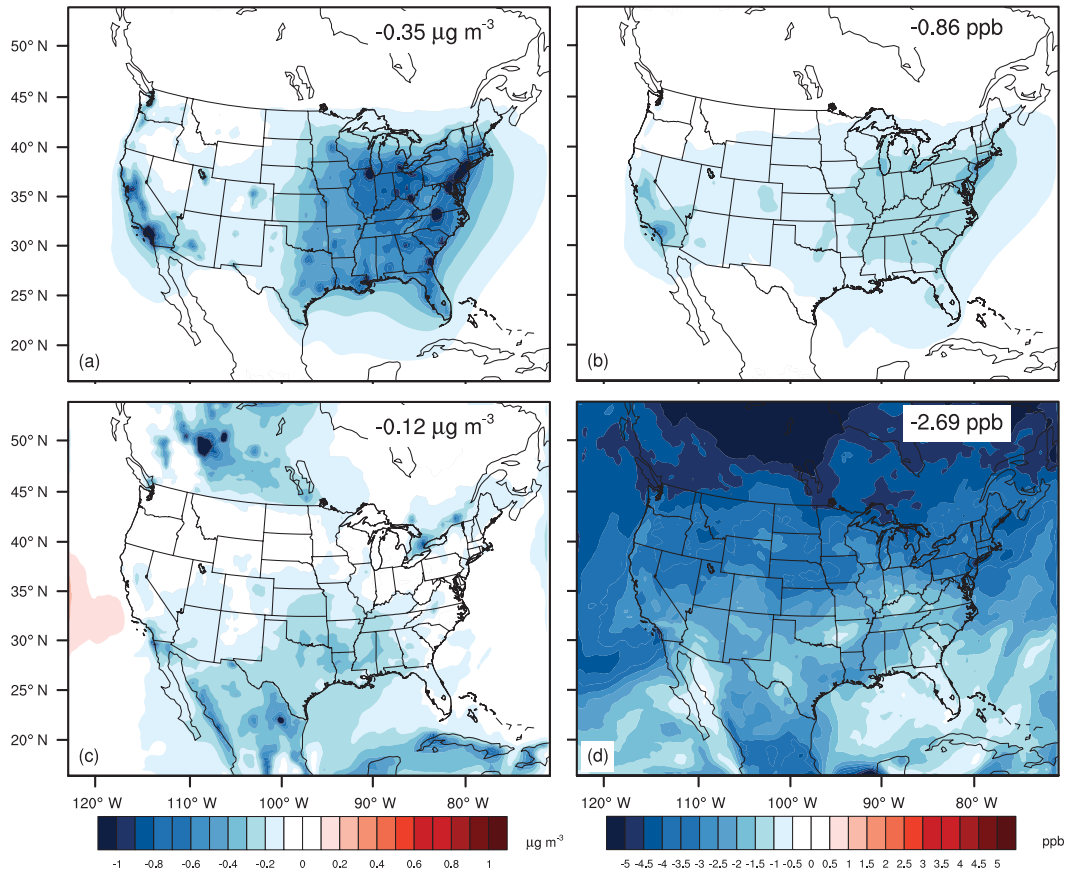

Figure 7. Benefits of domestic (**a**, **b**; S_Dom–S_REF) vs. foreign **(c, d)** GHG reductions for $PM_{2.5}$ (**a**, **c**; S_RCP45–S_Dom) and ozone season MDA8 surface O_3 **(b, d)**. Blue colors indicate an air quality improvement. The numbers on the plots are the 3-year average of air quality changes over the US.

For O_3, the northeast, east north central and northwest areas have the highest total co-benefits (regional means of 4.61, 4.25 and 4.15 ppb; Fig. 9 and Table S3), although the total co-benefits for O_3 are fairly uniform over the US (Fig. 5). The southeast has the lowest total co-benefits, with 2.67 ppb for the regional mean. Domestic co-benefits are higher over the center, northeast and southeast, with regional means of 1.25, 1.16 and 1.14 ppb, and lowest over the northwest (0.4 ppb). In general, foreign mitigation contributes more in the west than the east, most likely influenced by intercontinental transport from Asia. It is highest in the northwest, west north central and northeast areas, with regional means of 3.75, 3.45 and 3.45 ppb. The fraction of co-benefits from foreign mitigation is larger than 60 % in most regions, highest over the northwest (90 %) and lowest over the southeast (57 %).

We also evaluate the variability in co-benefits for the 3 years simulated (Table S3). Over the US, the coefficient of variation (CV) for the total co-benefits for $PM_{2.5}$ (7 %) is much lower than that of the total co-benefits for O_3 (37 %), which is controlled by the intercontinental transport and global CH_4. The southeast has the highest CV (29 %) for the total co-benefits of $PM_{2.5}$, while other regions are lower than 15 %, lowest in the east north central and northeast areas (3 %). The southwest and south have the highest CV (70, 69 %) for the total co-benefits of O_3 and the lowest in the northwest (21 %). For regions with higher variability, longer simulations would be desirable to better quantify the annual average co-benefits.

4 Discussion

The co-benefits we present here are specific to the reference (REF) and mitigation (RCP4.5) scenarios we choose, and results would differ for other baseline and mitigation scenarios. The estimated co-benefits also depend on the participation of many nations in the mitigation policies, and delaying participation will likely change the co-benefits. However, we expect that the general features of these results are generalizable to other scenarios.

The total co-benefits for O_3 when downscaled are comparable to the global study in both magnitude and spatial pattern, but the downscaled simulations capture some local fea-

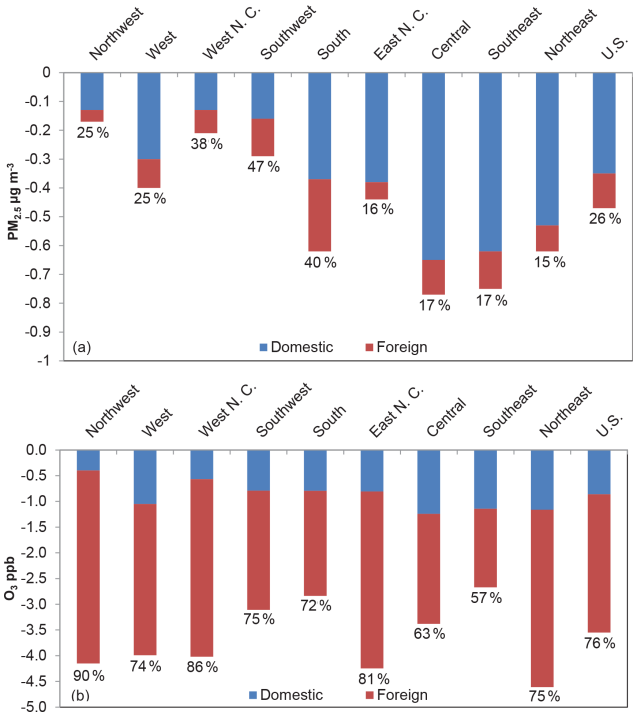

Figure 8. Mean values of domestic (blue) and foreign co-benefits (red) for US average **(a)** annual $PM_{2.5}$ and **(b)** ozone season MDA8 O_3. The numbers below each bar are the percentage (%) of the foreign co-benefit.

tures better than the global model, such as the effects of topography and urban areas. For $PM_{2.5}$, significant differences are seen from the downscaling due to the fine resolution and different chemical mechanisms between the global and the regional model. The resolution we are using for this study (36 by 36 km) is fine enough for us to analyze the co-benefits at a state level but insufficient to fully resolve urban areas. Finer-resolution simulations (such as 12 by 12 km) with CMAQ or other CTMs can be carried out to better quantify the co-benefits over urban areas.

For this study, uncertainties and errors may exist under the assumptions and choices we make for each model. For example, uncertainties in the input meteorology and emissions data inventory have a significant influence on the CMAQ results. Also, we see that the co-benefits of $PM_{2.5}$ have large contributions from OC and SOA over the central and east US (Figs. 4, S18). However, our model evaluations show that CMAQ greatly underestimates the total OC (primary OC and SOA) concentration compared with surface observations. New gas-phase and aqueous-phase oxidation pathways for SOA formation are found to play significant roles in producing organic aerosols (Lin et al., 2013; Pye and Pouliot, 2012; Pye et al., 2013), which are missing in the CMAQ version used in this study. We use the BEIS model to estimate the biogenic VOC (BVOC) emissions, but studies have shown that the BVOCs from the Model of Emissions of Gases and Aerosols from Nature (MEGAN) are higher than those from BEIS by a factor of 2 (Pouliot, 2008; Pouliot and Pierce, 2009), which highlights the uncertainty in representing these emissions and simulating both $PM_{2.5}$ and O_3 (Hogrefe et al., 2011).

We assume constant land use in the GCM, WRF and CMAQ when simulating the global and regional climate and estimating the biogenic emissions, which could introduce errors in our results (Unger, 2014; Heald and Spracklen, 2015). When we process the global anthropogenic emissions with SMOKE, we back-calculate the total $PM_{2.5}$ and PMC from OC and BC, which introduces inorganic PM emissions and may make our results for co-benefits of $PM_{2.5}$ higher. By doing this, we account for missing emissions but also increase the total uncertainties in the emission inventory. Spectral nudging is adopted in this study to restrain WRF from drifting from the GCM, which has been shown to be better for some meteorological variables, but analysis nudging is better for others (Bowden et al., 2012, 2013; Otte et al., 2012). Moreover, only one model is used during downscaling for regional climate (WRF) and air quality (CMAQ) modeling, and the mean of a model ensemble can be used to reduce model error. Simulations are based on 3-year averages, due to computational limitations, but these 3 years may reflect meteorological variability and not only climate change. This uncertainty may be greater for the total co-benefits of O_3, for which we see greater year-to-year variations than for $PM_{2.5}$. CMAQ simulations could be performed over more years to reduce the influence of the interannual climate variability. In separating domestic and foreign co-benefits, we assume that global and regional climate will be controlled by foreign GHG emissions and not influenced by GHG mitigation in the US, which introduces a small error into our results. We similarly attribute the global methane change to foreign influence, as US methane emissions are a small fraction (6–10 %) of global emissions.

5 Conclusions

Climate polices to control GHG emissions will not only have the benefit of slowing climate change but can also have co-benefits of improved air quality. Previous co-benefits studies focus mostly on local or regional GHG reductions. As a result, these studies omit air quality benefits outside of the domain considered and neglect benefits from global GHG mitigation. In this study we adopt a systematic approach to quantify the co-benefits from both the global and regional GHG mitigation for regional air quality over the US at fine resolution in 2050, building on the global co-benefits study from West et al. (2013). The co-benefits of global GHG mitigation for US air quality are discussed through two mechanisms: reduced co-emitted air pollutants and slowing climate change and its influence on air quality. We also quantify the

co-benefits from domestic GHG mitigation vs. foreign countries' reduction.

We find that there are significant benefits for both $PM_{2.5}$ and O_3 over the US by 2050 from the global GHG mitigation in RCP4.5. The total co-benefits for $PM_{2.5}$ are higher in the east than the west, with an average of $0.47\,\mu g\,m^{-3}$ over the US For O_3, the total co-benefits are fairly uniform across the US at 2–5 ppb, with a US average of 3.55 ppb. The co-benefits from reductions in co-emitted air pollutants have a greater influence on both $PM_{2.5}$ (accounting for 96 % of total decreases) and O_3 (89 % of the total decreases) than the second mechanism via slowing climate change, consistent with West et al. (2013).

Foreign countries' GHG reductions have a much greater influence on the US O_3 reduction (76 % of the total) compared with that from domestic GHG mitigation only (24 %), highlighting the importance of global methane reductions and the intercontinental transport of air pollutants. For $PM_{2.5}$, the benefits of foreign GHG control are less than domestic control but still a considerable portion of the total (26 %). We conclude that the US can gain significantly greater domestic air quality co-benefits by engaging with other nations for GHG control to combat climate change, especially for O_3. This also applies to other nations which can be expected to have ancillary air quality benefits from foreign countries' GHG mitigation. We also conclude that previous studies that estimate co-benefits for one nation or region (e.g., Thomson et al., 2014), may significantly underestimate the full co-benefits when many countries reduce GHGs together, particularly for O_3.

6 Data availability

Inputs and outputs of all model simulations are archived at UNC's mass storage system and can be obtained by contacting the corresponding author.

The Supplement related to this article is available online at doi:10.5194/acp-16-9533-2016-supplement.

Acknowledgements. This publication was financially supported by the US Environmental Protection Agency (USEPA) STAR grant no. 834285 and the National Institute of Environmental Health Sciences grant no. 1 R21 ES022600-01. Its contents are solely the responsibility of the grantee and do not necessarily represent the official views of the USEPA or other funding sources. USEPA and other funding sources do not endorse the purchase of any commercial products or services mentioned in the publication.

Edited by: Q. Zhang
Reviewed by: two anonymous referees

References

Appel, K. W., Bhave, P. V., Gilliland, A. B., Sarwar, G., and Roselle, S. J.: Evaluation of the community multiscale air quality (CMAQ) model version 4.5: Sensitivities impacting model performance; Part II-particulate matter, Atmos. Environ., 42, 6057–6066, doi:10.1016/j.atmosenv.2008.03.036, 2008.

Appel, K. W., Roselle, S. J., Gilliam, R. C., and Pleim, J. E.: Sensitivity of the Community Multiscale Air Quality (CMAQ) model v4.7 results for the eastern United States to MM5 and WRF meteorological drivers, Geosci. Model Dev., 3, 169–188, doi:10.5194/gmd-3-169-2010, 2010.

Appel, K. W., Foley, K. M., Bash, J. O., Pinder, R. W., Dennis, R. L., Allen, D. J., and Pickering, K.: A multi-resolution assessment of the Community Multiscale Air Quality (CMAQ) model v4.7 wet deposition estimates for 2002-2006, Geosci. Model Dev., 4, 357–371, doi:10.5194/gmd-4-357-2011, 2011.

Appel, K. W., Pouliot, G. A., Simon, H., Sarwar, G., Pye, H. O. T., Napelenok, S. L., Akhtar, F., and Roselle, S. J.: Evaluation of dust and trace metal estimates from the Community Multiscale Air Quality (CMAQ) model version 5.0, Geosci. Model Dev., 6, 883–899, doi:10.5194/gmd-6-883-2013, 2013.

Avise, J., Chen, J., Lamb, B., Wiedinmyer, C., Guenther, A., Salathé, E., and Mass, C.: Attribution of projected changes in summertime US ozone and $PM_{2.5}$ concentrations to global changes, Atmos. Chem. Phys., 9, 1111–1124, doi:10.5194/acp-9-1111-2009, 2009.

Bell, M. L., Davis, D. L., Cifuentes, L. A, Krupnick, A. J., Morgenstern, R. D., and Thurston, G. D.: Ancillary human health benefits of improved air quality resulting from climate change mitigation, Environ. Health, 7, 41, doi:10.1186/1476-069X-7-41, 2008.

Bowden, J. H., Otte, T. L., Nolte, C. G., and Otte, M. J.: Examining Interior Grid Nudging Techniques Using Two-Way Nesting in the WRF Model for Regional Climate Modeling, J. Climate, 25, 2805–2823, doi:10.1175/JCLI-D-11-00167.1, 2012.

Bowden, J. H., Nolte, C. G., and Otte, T. L.: Simulating the impact of the large-scale circulation on the 2 m temperature and precipitation climatology, Clim. Dynam., 40, 1903–1920, doi:10.1007/s00382-012-1440-y, 2013.

Byun, D. and Schere, K. L.: Review of the Governing Equations, Computational Algorithms, and Other Components of the Models-3 Community Multiscale Air Quality (CMAQ) Modeling System, Appl. Mech. Rev., 59, 51–77, doi:10.1115/1.2128636, 2006.

Chen, F. and Dudhia, J.: Coupling an Advanced Land Surface–Hydrology Model with the Penn State–NCAR MM5 Modeling System, Part I: Model Implementation and Sensitivity, Mon. Weather Rev., 129, 569–585, 2001.

Chen, J., Avise, J., Lamb, B., Salathé, E., Mass, C., Guenther, A., Wiedinmyer, C., Lamarque, J.-F., O'Neill, S., McKenzie, D., and Larkin, N.: The effects of global changes upon regional ozone pollution in the United States, Atmos. Chem. Phys., 9, 1125–1141, doi:10.5194/acp-9-1125-2009, 2009.

Cifuentes, L., Borja-aburto, V. H., Gouveia, N., Thurston, G., and Davis, D. L.: Hidden Health Benefits of Greenhouse Gas Mitigation, Science, 293, 1257–1259, 2001.

Donner, L. J., Wyman, B. L., Hemler, R. S., Horowitz, L. W., Ming, Y., Zhao, M., Golaz, J. C., Ginoux, P., Lin, S. J., Schwarzkopf, M. D., Austin, J., Alaka, G., Cooke, W. F., Delworth, T. L., Freiden-

reich, S. M., Gordon, C. T., Griffies, S. M., Held, I. M., Hurlin, W. J., Klein, S. A., Knutson, T. R., Langenhorst, A. R., Lee, H. C., Lin, Y., Magi, B. I., Malyshev, S. L., Milly, P. C. D., Naik, V., Nath, M. J., Pincus, R., Ploshay, J. J., Ramaswamy, V., Seman, C. J., Shevliakova, E., Sirutis, J. J., Stern, W. F., Stouffer, R. J., Wilson, R. J., Winton, M., Wittenberg, A. T., and Zeng, F.: The dynamical core, physical parameterizations, and basic simulation characteristics of the atmospheric component AM3 of the GFDL global coupled model CM3, J. Climate, 24, 3484–3519, doi:10.1175/2011JCLI3955.1, 2011.

Emmons, L. K., Walters, S., Hess, P. G., Lamarque, J.-F., Pfister, G. G., Fillmore, D., Granier, C., Guenther, A., Kinnison, D., Laepple, T., Orlando, J., Tie, X., Tyndall, G., Wiedinmyer, C., Baughcum, S. L., and Kloster, S.: Description and evaluation of the Model for Ozone and Related chemical Tracers, version 4 (MOZART-4), Geosci. Model Dev., 3, 43–67, doi:10.5194/gmd-3-43-2010, 2010.

Fiore, A. M., Naik, V., Spracklen, D. V, Steiner, A., Unger, N., Prather, M., Bergmann, D., Cameron-Smith, P. J., Cionni, I., Collins, W. J., Dalsøren, S. , Eyring, V., Folberth, G. A, Ginoux, P., Horowitz, L. W., Josse, B., Lamarque, J.-F., MacKenzie, I. A, Nagashima, T., O'Connor, F. M., Righi, M., Rumbold, S. T., Shindell, D. T., Skeie, R. B., Sudo, K., Szopa, S., Takemura, T., and Zeng, G.: Global air quality and climate, Chem. Soc. Rev., 41, 6663–83, doi:10.1039/c2cs35095e, 2012.

Fiore, A. M., Naik, V., and Leibensperger, E. M.: Air Quality and Climate Connections, J. Air Waste Manage. Assoc., 65, 645–685, doi:10.1080/10962247.2015.1040526, 2015.

Fountoukis, C. and Nenes, A.: ISORROPIA II: a computationally efficient thermodynamic equilibrium model for K^+–Ca^{2+}–Mg^{2+}–NH_4^+–Na^+–SO_4^{2-}–NO_3^-–Cl^-–H_2O aerosols, Atmos. Chem. Phys., 7, 4639–4659, doi:10.5194/acp-7-4639-2007, 2007.

Gao, Y., Fu, J. S., Drake, J. B., Lamarque, J.-F., and Liu, Y.: The impact of emission and climate change on ozone in the United States under representative concentration pathways (RCPs), Atmos. Chem. Phys., 13, 9607–9621, doi:10.5194/acp-13-9607-2013, 2013.

Grell, G. A. and Devenyi, D.: A generalized approach to parameterizing convection combining ensemble and data assimilation techniques, Geophys. Res. Lett., 29, 10–13, doi:10.1029/2002GL015311, 2002.

Heald, C. L. and Spracklen, D. V.: Land Use Change Impacts on Air Quality and Climate, Chem. Rev., 115, 4476–4496, doi:10.1021/cr500446g, 2015.

Higgins, R.W., Shi W., and Joyce, R.: Improved United States precipitation quality control system and analysis, NCEP/Climate Prediction Center ATLAS No. 7, 2000.

Hogrefe, C., Lynn, B., Civerolo, K., Ku, J.-Y., Rosenthal, J., Rosenzweig, C., Goldberg, R., Gaffin, S., Knowlton, K., and Kinney, P. L.: Simulating changes in regional air pollution over the eastern United States due to changes in global and regional climate and emissions, J. Geophys. Res., 109, D22301, doi:10.1029/2004JD004690, 2004.

Hogrefe, C., Isukapalli, S. S., Tang, X., Georgopoulos, P. G., He, S., Zalewsky, E. E., Hao, W., Ku, J.-Y., Key, T., and Sistla, G.: Impact of biogenic emission uncertainties on the simulated response of ozone and fine particulate matter to anthropogenic emission reductions, J. Air Waste Manag. Assoc., 61, 92–108, doi:10.3155/1047-3289.61.1.92, 2011.

Hong, S. and Lim, J.: The WRF single-moment 6-class microphysics scheme (WSM6), J. Korean Meteorol. Soc., 42, 129–151, 2006.

Hong, S.-Y., Noh, Y., and Dudhia, J.: A New Vertical Diffusion Package with an Explicit Treatment of Entrainment Processes, Mon. Weather Rev., 134, 2318–2341, doi:10.1175/MWR3199.1, 2006.

Houyoux, M. R., Vukovich, J. M., Coats Jr., C. J., Wheeler, N. J. M., and Kasibhatla, P. S.: Emission inventory development and processing for the Seasonal Model for Regional Air Quality (SMRAQ) project, J. Geophys. Res., 105, 9079–9090, 2000.

Iacono, M. J., Delamere, J. S., Mlawer, E. J., Shephard, M. W., Clough, S. A., and Collins, W. D.: Radiative forcing by long-lived greenhouse gases: Calculations with the AER radiative transfer models, J. Geophys. Res. Atmos., 113, 2–9, doi:10.1029/2008JD009944, 2008.

Jacob, D. J. and Winner, D. A.: Effect of climate change on air quality, Atmos. Environ., 43, 51–63, doi:10.1016/j.atmosenv.2008.09.051, 2009.

Kelly, J. T., Bhave, P. V., Nolte, C. G., Shankar, U., and Foley, K. M.: Simulating emission and chemical evolution of coarse sea-salt particles in the Community Multiscale Air Quality (CMAQ) model, Geosci. Model Dev., 3, 257–273, doi:10.5194/gmd-3-257-2010, 2010.

Lam, Y. F., Fu, J. S., Wu, S., and Mickley, L. J.: Impacts of future climate change and effects of biogenic emissions on surface ozone and particulate matter concentrations in the United States, Atmos. Chem. Phys., 11, 4789–4806, doi:10.5194/acp-11-4789-2011, 2011.

Lamarque, J.-F., Shindell, D. T., Josse, B., Young, P. J., Cionni, I., Eyring, V., Bergmann, D., Cameron-Smith, P., Collins, W. J., Doherty, R., Dalsoren, S., Faluvegi, G., Folberth, G., Ghan, S. J., Horowitz, L. W., Lee, Y. H., MacKenzie, I. A., Nagashima, T., Naik, V., Plummer, D., Righi, M., Rumbold, S. T., Schulz, M., Skeie, R. B., Stevenson, D. S., Strode, S., Sudo, K., Szopa, S., Voulgarakis, A., and Zeng, G.: The Atmospheric Chemistry and Climate Model Intercomparison Project (ACCMIP): overview and description of models, simulations and climate diagnostics, Geosci. Model Dev., 6, 179–206, doi:10.5194/gmd-6-179-2013, 2013.

Lin, Y.-H., Zhang, H., Pye, H. O. T., Zhang, Z., Marth, W. J., Park, S., Arashiro, M., Cui, T., Budisulistiorini, S. H., Sexton, K. G., Vizuete, W., Xie, Y., Luecken, D. J., Piletic, I. R., Edney, E. O., Bartolotti, L. J., Gold, A., and Surratt, J. D.: Epoxide as a precursor to secondary organic aerosol formation from isoprene photooxidation in the presence of nitrogen oxides., P. Natl. Acad. Sci. USA, 110, 6718–23, doi:10.1073/pnas.1221150110, 2013.

Mesinger, F., DiMego, G., Kalnay, E., Mitchell, K., Shafran, P. C., Ebisuzaki, W., Jovic, D., Woollen, J., Rogers, E., Berbery ,E.H., Ek M. B., Fan, Y., Grumbine, R., Higgins, W., Li, H., Lin, Y., Manikin, G., Parrish, D., and Shi, W.: North American regional reanalysis, B. Am. Meteorol. Soc., 87, 343–360, 2006.

Myhre, G., Shindell, D., Bréon, F.-M., Collins, W., Fuglestvedt, J., Huang, J., Koch, D., Lamarque, J.-F., Lee, D., Mendoza, B., Nakajima, T., Robock, A., Stephens, G., Takemura, T., and Zhang, H.: Anthropogenic and Natural Radiative Forcing, in: Climate Change 2013: The Physical Science Basis, Contribution

of Working Group I to the Fifth Assessment Report of the Intergovernmental Panel on Climate Change, edited by: Stocker, T. F., Qin, D., Plattner, G.-K., Tignor, M., Allen, S. K., Boschung, J., Nauels, A., Xia, Y., Bex, V., and Midgley, P. M., Cambridge University Press, Cambridge, United Kingdom and New York, NY, USA, 659–740, doi:10.1017/CBO9781107415324.018, 2013.

Naik, V., Horowitz, L. W., Fiore, A. M., Ginoux, P., Mao, J., Aghedo, A. M., and Levy, H.: Impact of preindustrial to present-day changes in short-lived pollutant emissions on atmospheric composition and climate forcing, J. Geophys. Res. Atmos., 118, 8086–8110, doi:10.1002/jgrd.50608, 2013.

Nakicenovic, N. and Swart, R.: Special Report on Emissions Scenarios: A Special Report of Working Group III of the Intergovernmental Panel on Climate Change, Cambridge University Press, Cambridge, United Kingdom and New York, NY, USA, 2000.

Nemet, G. F., Holloway, T., and Meier, P.: Implications of incorporating air-quality co-benefits into climate change policymaking, Environ. Res. Lett., 5, 014007, doi:10.1088/1748-9326/5/1/014007, 2010.

Nolte, C. G., Gilliland, A. B., Hogrefe, C., and Mickley, L. J.: Linking global to regional models to assess future climate impacts on surface ozone levels in the United States, J. Geophys. Res., 113, D14307, doi:10.1029/2007JD008497, 2008.

Nolte, C. G., Appel, K. W., Kelly, J. T., Bhave, P. V., Fahey, K. M., Collett Jr., J. L., Zhang, L., and Young, J. O.: Evaluation of the Community Multiscale Air Quality (CMAQ) model v5.0 against size-resolved measurements of inorganic particle composition across sites in North America, Geosci. Model Dev., 8, 2877–2892, doi:10.5194/gmd-8-2877-2015, 2015.

Otte, T. L. and Pleim, J. E.: The Meteorology-Chemistry Interface Processor (MCIP) for the CMAQ modeling system: updates through MCIPv3.4.1, Geosci. Model Dev., 3, 243–256, doi:10.5194/gmd-3-243-2010, 2010.

Otte, T. L., Nolte, C. G., Otte, M. J., and Bowden, J. H.: Does Nudging Squelch the Extremes in Regional Climate Modeling?, J. Climate, 25, 7046–7066, doi:10.1175/JCLI-D-12-00048.1, 2012.

Pouliot, G.: A Tale of Two Models: A Comparison of the Biogenic Emission Inventory System (BEIS3.14) and Model of Emissions of Gases and Aerosols from Nature (MEGAN 2.04), 7th Annual CMAS Conference, Chapel Hill, NC, USA, 7 October 2008.

Pouliot, G. and Pierce, T. E.: Integration of the Model of Emissions of Gases and Aerosols from Nature (MEGAN) into the CMAQ Modeling System, 18th International Emission Inventory Conference, Baltimore, Maryland, 14–17 April 2009.

Pye, H. O. T. and Pouliot, G. A: Modeling the Role of Alkanes, Polycyclic Aromatic Hydrocarbons, and Their Oligomers in Secondary Organic Aerosol Formation, Environ. Sci. Technol., 46, 6041–6047, doi:10.1021/es300409w, 2012.

Pye, H. O. T., Pinder, R. W., Piletic, I. R., Xie, Y., Capps, S. L., Lin, Y. H., Surratt, J. D., Zhang, Z., Gold, A., Luecken, D. J., Hutzell, W. T., Jaoui, M., Offenberg, J. H., Kleindienst, T. E., Lewandowski, M., and Edney, E. O.: Epoxide pathways improve model predictions of isoprene markers and reveal key role of acidity in aerosol formation, Environ. Sci. Technol., 47, 11056–11064, doi:10.1021/es402106h, 2013.

Reff, A., Bhave, P. V, Simon, H., Pace, T. G., Pouliot, G. A., Mobley, J. D., and Houyoux, M.: Emissions Inventory of $PM_{2.5}$ Trace Elements across the United States, Environ. Sci. Technol., 43, 5790–5796, doi:10.1021/es802930x, 2009.

Simon, H. and Bhave, P. V.: Simulating the degree of oxidation in atmospheric organic particles, Environ. Sci. Technol., 46, 331–339, doi:10.1021/es202361w, 2012.

Skamarock, W. C. and Klemp, J. B.: A time-split nonhydrostatic atmospheric model for weather research and forecasting applications, J. Comput. Phys., 227, 3465–3485, doi:10.1016/j.jcp.2007.01.037, 2008.

Tagaris, E., Manomaiphiboon, K., Liao, K.-J., Leung, L. R., Woo, J.-H., He, S., Amar, P., and Russell, A. G.: Impacts of global climate change and emissions on regional ozone and fine particulate matter concentrations over the United States, J. Geophys. Res., 112, D14312, doi:10.1029/2006JD008262, 2007.

Tai, A. P. K., Mickley, L. J., and Jacob, D. J.: Correlations between fine particulate matter ($PM_{2.5}$) and meteorological variables in the United States: Implications for the sensitivity of $PM_{2.5}$ to climate change, Atmos. Environ., 44, 3976–3984, doi:10.1016/j.atmosenv.2010.06.060, 2010.

Thomson, A. M., Calvin, K. V., Smith, S. J., Kyle, G. P., Volke, A., Patel, P., Delgado-Arias, S., Bond-Lamberty, B., Wise, M. A., Clarke, L. E., and Edmonds, J. A.: RCP4.5: A pathway for stabilization of radiative forcing by 2100, Climate Change, 109, 77–94, doi:10.1007/s10584-011-0151-4, 2011.

Thompson, T. M., Rausch, S., Saari, R. K., and Selin, N. E.: A systems approach to evaluating the air quality co-benefits of US carbon policies, Nature Climate Change, 4, 917–923, doi:10.1038/nclimate2342, 2014.

Trail, M. A., Tsimpidi, A. P., Liu, P., Tsigaridis, K., Hu, Y., Rudokas, J. R., Miller, P. J., Nenes, A., and Russell, A. G.: Impacts of Potential CO_2-Reduction Policies on Air Quality in the United States, Environ. Sci. Technol., 49, 5133–5141, doi:10.1021/acs.est.5b00473, 2015.

Unger, N.: Human land-use-driven reduction of forest volatiles cools global climate, Nature Climate Change, 4, 907–910, doi:10.1038/NCLIMATE2347, 2014.

US Environmental Protection Agency: Guidance on the Use of Models and Other Analyses for Demonstrating Attainment of Air Quality Goals for Ozone, $PM_{2.5}$ and Regional Haze, EPA-454/B-07e002, 2007.

Van Vuuren, D. P., Edmonds, J., Kainuma, M., Riahi, K., Thomson, A., Hibbard, K., Hurtt, G. C., Kram, T., Krey, V., Lamarque, J. F., Masui, T., Meinshausen, M., Nakicenovic, N., Smith, S. J., and Rose, S. K.: The representative concentration pathways: An overview, Climate Change, 109, 5–31, doi:10.1007/s10584-011-0148-z, 2011.

Weaver, C. P., Cooter, E., Gilliam, R., Gilliland, A., Grambsch, A., Grano, D., Hemming, B., Hunt, S. W., Nolte, C., Winner, D. A., Liang, X.-Z., Zhu, J., Caughey, M., Kunkel, K., Lin, J.-T., Tao, Z., Williams, A., Wuebbles, D. J., Adams, P. J., Dawson, J. P., Amar, P., He, S., Avise, J., Chen, J., Cohen, R. C., Goldstein, A. H., Harley, R. A., Steiner, A. L., Tonse, S., Guenther, A., Lamarque, J.-F., Wiedinmyer, C., Gustafson, W. I., Leung, L. R., Hogrefe, C., Huang, H.-C., Jacob, D. J., Mickley, L. J., Wu, S., Kinney, P. L., Lamb, B., Larkin, N. K., McKenzie, D., Liao, K.-J., Manomaiphiboon, K., Russell, A. G., Tagaris, E., Lynn, B. H., Mass, C., Salathé, E., O'neill, S. M., Pandis, S. N., Racherla, P. N., Rosenzweig, C., and Woo, J.-H.: A Preliminary Synthesis of Modeled Climate Change Impacts on US Regional

Ozone Concentrations, B. Am. Meteorol. Soc., 90, 1843–1863, doi:10.1175/2009BAMS2568.1, 2009.

West, J. J., Smith, S. J., Silva, R. A, Naik, V., Zhang, Y., Adelman, Z., Fry, M. M., Anenberg, S., Horowitz, L. W., and Lamarque, J.-F.: Co-benefits of Global Greenhouse Gas Mitigation for Future Air Quality and Human Health, Nature Climate Change, 3, 885–889, doi:10.1038/NCLIMATE2009, 2013.

Wu, S., Mickley, L. J., Leibensperger, E. M., Jacob, D. J., Rind, D., and Streets, D. G.: Effects of 2000–2050 global change on ozone air quality in the United States, J. Geophys. Res., 113, D06302, doi:10.1029/2007JD008917, 2008.

Xing, J., Pleim, J., Mathur, R., Pouliot, G., Hogrefe, C., Gan, C.-M., and Wei, C.: Historical gaseous and primary aerosol emissions in the United States from 1990 to 2010, Atmos. Chem. Phys., 13, 7531–7549, doi:10.5194/acp-13-7531-2013, 2013.